Simulating Virtual Terminal Area Weather Data Bases for Use in the Wake Vortex Avoidance System (Wake VAS) Prediction Algorithm

NAG1-03043 Final Research Grant Report
NASA-Langley Research Center
Hampton, Virginia 23681-2199
ATTN: Fred H. Proctor

Michael L. Kaplan* and Yuh-Lang Lin
Department of Marine, Earth and Atmospheric Sciences
North Carolina State University
Raleigh, North Carolina 27695-8208

December 2004

*Michael L. Kaplan, Department of Marine, Earth and Atmospheric Sciences, North Carolina State University, Raleigh, North Carolina 27695-8208, E-MAIL:

mlkaplan@unity.ncsu.edu, PHONE:919-515-1442, FAX:919-481-9332.

1. Summary of the Research

During the research project, sounding datasets were generated for the region surrounding 9 major airports, including Dallas, TX, Boston, MA, New York, NY, Chicago, IL, St. Louis, MO, Atlanta, GA, Miami, FL, San Francico, CA, and Los Angeles, CA. The numerical simulation of winter and summer environments during which no instrument flight rule impact was occurring at these 9 terminals was performed using the most contemporary version of the Terminal Area PBL Prediction System (TAPPS) model nested from 36 km to 6 km to 1 km horizontal resolution and very detailed vertical resolution in the planetary boundary layer (e.g, note Appendix A). The soundings from the 1 km model were archived at 30 minute time intervals for a 24 hour period and the vertical dependent variables as well as derived quantities, i.e., 3-dimensional wind components, temperatures, pressures, mixing ratios, turbulence kinetic energy and eddy dissipation rates were then interpolated to 5 m vertical resolution up to 1000 m elevation above ground level. After partial validation against field experiment datasets for Dallas as well as larger scale and much coarser resolution observations at the other 8 airports, these sounding datasets were sent to NASA for use in the Virtual Air Space and Modeling program. The application of these datasets being to determine representative airport weather environments to diagnose the response of simulated wake vortices to realistic atmospheric environments. These virtual datasets are based on large scale observed atmospheric initial conditions that are dynamically interpolated in space and time employing a numerical simulation model based on a comprehensive hydro-thermodynamical equation set. The 1 km nested-grid simulated datasets providing a very coarse and highly smoothed representation of airport environment meteorological conditions. Details concerning the airport surface forcing are virtually absent from these simulated datasets although the observed background atmospheric processes have been compared to the simulated fields and the fields were found to accurately replicate the flows surrounding the airport where coarse verification data were available as well as where airport scale datasets where available at Dallas (e,g., note Appendix A). The simulated profiles of atmospheric dependent variables can be viewed online at the following links:
1) http://mesolab.meas.ncsu.edu/%7Eamhoggarth/wakevortex/wake_research.html , 2) http://mesolab.meas.ncsu.edu/~mtk3581/wake/ , 3) http://mesolab.meas.ncsu.edu/~paul/
.

Appendix A

Simulating Virtual Terminal Area Weather Data Bases for Use in the Wake Vortex Advisory System – Dallas-Fort Worth Wake-VAS Preliminary Simulation Experiments

NAG1-0343 Research Task Report for Summer 2004
NASA-Langley Research Center
Hampton, Virginia 23681-2199
ATTN: David K. Rutishauser

Michael L. Kaplan* and Yuh-Lang Lin
Department of Marine, Earth and Atmospheric Sciences
North Carolina State University
Raleigh, North Carolina 27695-8208

September 2004

*Michael Kaplan, Department of Marine, Earth and Atmospheric Sciences, North Carolina State University, Raleigh, NC, 27695-8208, E-MAIL:mlkaplan@unity.ncsu.edu, PHONE:919-515-1442, FAX:919-515-1683.

1. Task Overview

This report summarizes research on the development of virtual atmosphere sounding data sets for the Wake-Vortex Advisory System (Wake-VAS) during the summer of 2004. During this period the focus was on generating virtual sounding data sets at Dallas-Fort Worth International Airport (DFW) during the September 1997 AVOSS deployment. Soundings generated by the NHMASS 6.2 model, i.e., the Terminal Area PBL Prediction System (TAPPS), where directly compared to MIT Lincoln Laboratory synthesized observed soundings of u and v wind components as well as observations of 40 m eddy dissipation rate and turbulence kinetic energy at DFW. The comparison would represent evaluations of potential control simulations in anticipation of more complex future simulation studies. This represents precursor analyses in preparation for future simulation experiments in which local observations would be assimilated into the predictive system. These simulated soundings have highly detailed vertical structure for use in diagnosing realistic vertical wind shears, temperature lapse rates and, therefore, potential turbulence generating features in the planetary boundary layer at the DFW airport. The simulations were validated against the MIT observations to diagnose the status of their existing utility as components of a future Wake-VAS predictive system.

2. Modeling System/Numerical Simulation Experiments

The numerical model, NHMASS 6.2, is a nonhydrostatic and terrain following simulation model. This is a nonhydrostatic version of the Terminal Area PBL Prediction System (TAPPS) (Kaplan et al. 2000). The model lid was set at 100 hPa with focused vertical resolution below 1000 m elevation above ground level (AGL). The version of NHMASS employed for these simulation experiments included a 1.5 order prognostic turbulence kinetic energy planetary boundary layer formulation after Therry and Lacarrere (1983) and a convective parameterization scheme after Kain and Fritsch (1992). A comprehensive surface energy budget and soil moisture predictive scheme is utilized in the numerical model so that diurnal radiative forcing of the earth's surface and hydrological forcing is included in the surface layer of the simulated atmosphere (Mahrt and Pan 1984). Surface soil moisture was set at a climatological value for September in Dallas and land use/land cover databases as well as surface albedo where also generated based on prescribed datasets (Anderson et al. 1976; Noilan and Planton 1989). The eddy dissipation rate formulation (ε) employed in diagnostic calculations is consistent with that utilized in the turbulence kinetic energy boundary layer formulation. It is represented by the following expression from Bougeault and Lacarrere (1989) and Therry and Lacarrere (1983):

$$\varepsilon = Ce^{3/2}/\lambda\varepsilon \qquad (1)$$

where:

e = first guess turbulence kinetic energy derived from the full time dependent equation

C• = a first order numerical coefficient

•• = a characteristic length scale of the energy-containing eddies

The value of this characteristic length scale (••) is primarily a function of Richardson number wherein numerous thresholds exist for differing stability and shear regimes in order to differentiate the mixing length of eddies in stable, convective and transitional boundary layers.

The numerical experiments consisted of performing several one-way doubly-nested numerical simulations with NHMASS 6.2 during the September 1997 AVOSS deployment in the Dallas-Fort Worth, Texas metropolitan region. The simulations were centered on DFW. Three numerical grids were employed for these experiments: 1) 36 km horizontal resolution, 2) 6 km horizontal resolution and 3) 1 km horizontal resolution. Matrices included a 100 x 100 x 59, 50 x 50 x 59 and 25 x 25 x 59 grid, respectively, with very detailed and identical vertical resolution within the first 1000 m AGL of the numerical model for all 3 grids. The time periods of integration for the 3 grids were 24 hours, 24 hours and 30 minutes regenerated for the entire 24-hour period, respectively. This means that every 30 minutes a 1 km horizontal resolution simulation was performed from the 6 km simulated initial and lateral boundary condition data. The 6 km initial and lateral boundary conditions were derived from the 36 km simulation, which, in turn received its initial and lateral boundary conditions from NWS ETA gridded analyses, which were reanalyzed with synoptic scale rawinsondes as well as ASOS surface observations. No local (special AVOSS) DFW observations were utilized in the numerical simulations. The initial and lateral boundary condition datasets were solely derived from the NWS ETA analyses gridded fields as well as reanalyzed standard rawinsonde and aviation surface datasets. The simulations were initialized at 8 different time periods, i.e., 0000 UTC 16, 17, 18 and 19 September 1997 (group #1) and 1200 UTC 16, 17, 18 and 19 September 1997 (group #2). The groupings would allow statistical comparisons of the relative accuracy of the simulations comparing 0000 and 1200 UTC initialization times. Vertical soundings were constructed centered on DFW every 30 minutes from the 1 km simulations and interpolated to 5 m vertical resolution for comparison to the available observed fields at 200 levels up to 1000 m AGL. These simulated soundings included the following variables: 1) pressure (hPa), 2) height (m AGL), 3) temperature (K), 4) dew point temperature (K), 5) u wind component (m/s), 6) v wind component (m/s), 7) w wind component (m/s), 8) turbulence kinetic energy (m^2/s^2) and 9) eddy dissipation rate (m^2/s^3). These were sent to NASA-Langley for potential use in the Virtual Air Space Modeling Program. Figure 1, below, represents an example of one of these 384 soundings.

P(mb)	Z(m)	T(K)	TD(K)	U(m/s)	V(m/s)	W(m/s)	TKE	TKED
995.142	5.00000	300.615	294.579	-2.29894	-.389851	-.136917E-01	0.100000E-03	0.00000
994.577	10.0000	300.622	294.568	-2.30653	-.332376	-.144184E-01	0.281843E-01	0.431458E-03
994.012	15.0000	300.631	294.551	-2.30987	-.240490	-.152993E-01	0.574212E-01	0.849109E-03
993.447	20.0000	300.644	294.526	-2.30443	-.105129	-.161579E-01	0.758775E-01	0.102403E-02
992.883	25.0000	300.661	294.491	-2.28772	0.761115E-01	-.169777E-01	0.821731E-01	0.934865E-03
992.319	30.0000	300.672	294.454	-2.25700	0.269599	-.177050E-01	0.809197E-01	0.731693E-03
991.755	35.0000	300.666	294.421	-2.20826	0.442406	-.182775E-01	0.761870E-01	0.555970E-03

991.192	40.0000	300.646	294.394	-2.14447	0.587835	-.187137E-01	0.711182E-01	0.448001E-03
990.629	45.0000	300.617	294.370	-2.07236	0.713316	-.190768E-01	0.685720E-01	0.392788E-03
990.066	50.0000	300.585	294.350	-1.99717	0.823573	-.194162E-01	0.714182E-01	0.381731E-03
989.504	55.0000	300.550	294.331	-1.92102	0.923215	-.197466E-01	0.794071E-01	0.402202E-03
988.942	60.0000	300.512	294.314	-1.84439	1.01648	-.200634E-01	0.908216E-01	0.440239E-03
988.380	65.0000	300.472	294.297	-1.76767	1.10658	-.203600E-01	0.104461	0.484739E-03
987.818	70.0000	300.428	294.282	-1.69116	1.19515	-.206360E-01	0.119178	0.529359E-03
987.256	75.0000	300.383	294.267	-1.61515	1.28225	-.208995E-01	0.133612	0.572433E-03
986.695	80.0000	300.337	294.252	-1.53997	1.36765	-.211575E-01	0.146335	0.612339E-03
986.134	85.0000	300.293	294.237	-1.46603	1.45094	-.214152E-01	0.156033	0.647493E-03
985.573	90.0000	300.249	294.222	-1.39333	1.53228	-.216716E-01	0.163891	0.679738E-03
985.013	95.0000	300.205	294.207	-1.32178	1.61194	-.219229E-01	0.172154	0.712358E-03
984.452	100.000	300.158	294.192	-1.25147	1.68989	-.221645E-01	0.183138	0.748705E-03
983.892	105.000	300.107	294.178	-1.18261	1.76597	-.223914E-01	0.198884	0.791624E-03
983.332	110.000	300.053	294.164	-1.11498	1.84049	-.226055E-01	0.217562	0.837848E-03
982.772	115.000	299.999	294.149	-1.04831	1.91379	-.228103E-01	0.235995	0.881827E-03
982.213	120.000	299.946	294.135	-.982475	1.98602	-.230077E-01	0.250960	0.917638E-03
981.654	125.000	299.895	294.121	-.917500	2.05719	-.231985E-01	0.258848	0.938368E-03
981.095	130.000	299.847	294.107	-.853308	2.12737	-.233827E-01	0.259168	0.942715E-03
980.536	135.000	299.801	294.092	-.789728	2.19679	-.235597E-01	0.254631	0.935077E-03
979.977	140.000	299.755	294.078	-.726673	2.26554	-.237279E-01	0.247366	0.918305E-03
979.419	145.000	299.711	294.063	-.664144	2.33360	-.238840E-01	0.239060	0.893774E-03
978.861	150.000	299.665	294.049	-.602210	2.40090	-.240237E-01	0.231152	0.861795E-03
978.303	155.000	299.619	294.035	-.540820	2.46747	-.241471E-01	0.224016	0.823924E-03
977.745	160.000	299.573	294.020	-.479858	2.53348	-.242571E-01	0.217366	0.782485E-03
977.188	165.000	299.526	294.006	-.419275	2.59897	-.243545E-01	0.210973	0.739267E-03
976.631	170.000	299.480	293.991	-.359085	2.66390	-.244382E-01	0.204652	0.695768E-03
976.074	175.000	299.433	293.977	-.299358	2.72818	-.245048E-01	0.198232	0.653421E-03
975.517	180.000	299.386	293.962	-.240105	2.79177	-.245537E-01	0.191590	0.612834E-03
974.961	185.000	299.339	293.946	-.181210	2.85483	-.245892E-01	0.184664	0.573457E-03
974.405	190.000	299.293	293.931	-.122605	2.91745	-.246140E-01	0.177352	0.534827E-03
973.849	195.000	299.246	293.916	-.642646E-01	2.97965	-.246291E-01	0.169488	0.496603E-03
973.293	200.000	299.200	293.901	-.620795E-02	3.04137	-.246338E-01	0.160822	0.458509E-03
972.737	205.000	299.154	293.886	0.515062E-01	3.10251	-.246262E-01	0.151004	0.420317E-03
972.182	210.000	299.109	293.872	0.108893	3.16308	-.246064E-01	0.140254	0.382435E-03
971.627	215.000	299.063	293.858	0.166037	3.22321	-.245768E-01	0.129356	0.345937E-03
971.072	220.000	299.018	293.843	0.222990	3.28298	-.245383E-01	0.119101	0.312143E-03
970.517	225.000	298.972	293.829	0.279772	3.34241	-.244905E-01	0.110384	0.282812E-03
969.963	230.000	298.925	293.815	0.336376	3.40146	-.244313E-01	0.104346	0.260423E-03
969.409	235.000	298.878	293.801	0.392764	3.46003	-.243569E-01	0.102560	0.248570E-03
968.855	240.000	298.830	293.787	0.448918	3.51806	-.242643E-01	0.106128	0.249807E-03
968.301	245.000	298.780	293.772	0.504933	3.57568	-.241585E-01	0.113385	0.260190E-03
967.748	250.000	298.731	293.758	0.560917	3.63303	-.240442E-01	0.122560	0.275591E-03
967.195	255.000	298.681	293.744	0.616970	3.69024	-.239248E-01	0.132190	0.292692E-03
966.641	260.000	298.632	293.729	0.673204	3.74736	-.238031E-01	0.140889	0.308451E-03
966.089	265.000	298.584	293.714	0.729760	3.80446	-.236811E-01	0.147116	0.319607E-03
965.536	270.000	298.536	293.699	0.786831	3.86160	-.235610E-01	0.148937	0.322159E-03
964.984	275.000	298.490	293.683	0.844569	3.91883	-.234445E-01	0.144869	0.313053E-03
964.432	280.000	298.446	293.667	0.902816	3.97611	-.233299E-01	0.136401	0.295207E-03
963.880	285.000	298.402	293.651	0.961409	4.03340	-.232157E-01	0.125123	0.271752E-03
963.328	290.000	298.359	293.634	1.02024	4.09065	-.231000E-01	0.112170	0.244917E-03
962.777	295.000	298.316	293.617	1.07925	4.14781	-.229810E-01	0.984097E-01	0.216383E-03
962.226	300.000	298.273	293.601	1.13838	4.20482	-.228562E-01	0.845768E-01	0.187558E-03
961.675	305.000	298.230	293.585	1.19763	4.26160	-.227220E-01	0.713958E-01	0.159804E-03
961.124	310.000	298.187	293.569	1.25699	4.31801	-.225737E-01	0.596892E-01	0.134641E-03
960.573	315.000	298.144	293.553	1.31644	4.37398	-.224092E-01	0.498793E-01	0.112862E-03
960.023	320.000	298.100	293.538	1.37587	4.42953	-.222328E-01	0.415432E-01	0.937316E-04
959.473	325.000	298.056	293.522	1.43518	4.48466	-.220479E-01	0.343768E-01	0.767279E-04
958.923	330.000	298.012	293.508	1.49424	4.53927	-.218567E-01	0.282644E-01	0.616725E-04
958.374	335.000	297.968	293.493	1.55289	4.59320	-.216601E-01	0.232604E-01	0.487007E-04
957.825	340.000	297.923	293.479	1.61089	4.64618	-.214583E-01	0.195981E-01	0.382840E-04
957.276	345.000	297.878	293.465	1.66790	4.69775	-.212506E-01	0.177269E-01	0.313063E-04
956.727	350.000	297.831	293.451	1.72343	4.74728	-.210355E-01	0.183854E-01	0.292058E-04
956.178	355.000	297.783	293.439	1.77683	4.79389	-.208105E-01	0.225683E-01	0.339155E-04
955.630	360.000	297.733	293.427	1.82832	4.83784	-.205772E-01	0.299181E-01	0.447712E-04
955.082	365.000	297.683	293.416	1.87860	4.88004	-.203397E-01	0.392834E-01	0.595899E-04
954.534	370.000	297.632	293.405	1.92820	4.92112	-.201013E-01	0.498135E-01	0.767803E-04
953.986	375.000	297.581	293.394	1.97754	4.96156	-.198652E-01	0.608451E-01	0.951335E-04
953.439	380.000	297.531	293.382	2.02701	5.00169	-.196353E-01	0.717963E-01	0.113628E-03
952.891	385.000	297.481	293.369	2.07700	5.04184	-.194160E-01	0.820719E-01	0.131267E-03
952.344	390.000	297.433	293.356	2.12799	5.08231	-.192137E-01	0.909679E-01	0.146911E-03
951.797	395.000	297.386	293.340	2.18062	5.12348	-.190376E-01	0.975575E-01	0.159105E-03
951.251	400.000	297.342	293.321	2.23582	5.16580	-.189009E-01	0.100545	0.165836E-03
950.704	405.000	297.302	293.298	2.29414	5.20959	-.188116E-01	0.991236E-01	0.165849E-03
950.158	410.000	297.265	293.273	2.35475	5.25450	-.187561E-01	0.944914E-01	0.160952E-03
949.613	415.000	297.230	293.245	2.41690	5.30022	-.187216E-01	0.877460E-01	0.152801E-03
949.067	420.000	297.196	293.216	2.48008	5.34656	-.186987E-01	0.796446E-01	0.142525E-03
948.522	425.000	297.164	293.185	2.54394	5.39343	-.186798E-01	0.707253E-01	0.130912E-03
947.976	430.000	297.134	293.151	2.60826	5.44085	-.186582E-01	0.613944E-01	0.118535E-03
947.432	435.000	297.106	293.116	2.67287	5.48892	-.186264E-01	0.519920E-01	0.105841E-03
946.887	440.000	297.082	293.076	2.73767	5.53781	-.185755E-01	0.428465E-01	0.932285E-04
946.343	445.000	297.062	293.032	2.80257	5.58787	-.184935E-01	0.343276E-01	0.811081E-04
945.799	450.000	297.049	292.980	2.86750	5.63962	-.183634E-01	0.269063E-01	0.699698E-04
945.255	455.000	297.046	292.918	2.93242	5.69372	-.181642E-01	0.211346E-01	0.603702E-04
944.712	460.000	297.050	292.846	2.99726	5.74987	-.179032E-01	0.168534E-01	0.521773E-04
944.169	465.000	297.061	292.769	3.06192	5.80735	-.176006E-01	0.135799E-01	0.449457E-04
943.626	470.000	297.075	292.686	3.12632	5.86563	-.172702E-01	0.109871E-01	0.383783E-04
943.083	475.000	297.093	292.601	3.19030	5.92434	-.169211E-01	0.885759E-02	0.322855E-04
942.541	480.000	297.112	292.514	3.25364	5.98313	-.165596E-01	0.704902E-02	0.265537E-04
942.000	485.000	297.132	292.425	3.31603	6.04171	-.161899E-01	0.547059E-02	0.211281E-04
941.458	490.000	297.154	292.334	3.37698	6.09973	-.158149E-01	0.406865E-02	0.160028E-04
940.917	495.000	297.177	292.241	3.43579	6.15676	-.154366E-01	0.281804E-02	0.112208E-04
940.377	500.000	297.201	292.147	3.49141	6.21220	-.150566E-01	0.171799E-02	0.687999E-05

939.836	505.000	297.227	292.049	3.54228	6.26520	-.146761E-01	0.792035E-03	0.314978E-05
939.296	510.000	297.255	291.948	3.58607	6.31452	-.142962E-01	0.917275E-04	0.297754E-06
938.757	515.000	297.286	291.841	3.62108	6.35925	-.139179E-01	0.00000	0.00000
938.217	520.000	297.319	291.731	3.64949	6.40052	-.135413E-01	0.00000	0.00000
937.679	525.000	297.353	291.619	3.67342	6.43941	-.131669E-01	0.00000	0.00000
937.140	530.000	297.388	291.505	3.69423	6.47661	-.127952E-01	0.00000	0.00000
936.602	535.000	297.424	291.390	3.71279	6.51256	-.124273E-01	0.00000	0.00000
936.064	540.000	297.459	291.275	3.72962	6.54746	-.120651E-01	0.00000	0.00000
935.527	545.000	297.495	291.160	3.74495	6.58137	-.117110E-01	0.00000	0.00000
934.990	550.000	297.530	291.045	3.75877	6.61419	-.113690E-01	0.00000	0.00000
934.453	555.000	297.565	290.931	3.77082	6.64563	-.110451E-01	0.00000	0.00000
933.917	560.000	297.599	290.818	3.78056	6.67518	-.107481E-01	0.00000	0.00000
933.381	565.000	297.631	290.708	3.78707	6.70204	-.104910E-01	0.00000	0.00000
932.846	570.000	297.661	290.601	3.78893	6.72496	-.102936E-01	0.392815E-04	0.145830E-06
932.311	575.000	297.686	290.500	3.78396	6.74207	-.101847E-01	0.114231E-03	0.452396E-06
931.776	580.000	297.708	290.404	3.77108	6.75243	-.101791E-01	0.160931E-03	0.641052E-06
931.241	585.000	297.726	290.313	3.75250	6.75792	-.102481E-01	0.187237E-03	0.744605E-06
930.707	590.000	297.742	290.225	3.73009	6.76014	-.103675E-01	0.199867E-03	0.791122E-06
930.174	595.000	297.757	290.139	3.70507	6.76012	-.105215E-01	0.203335E-03	0.799468E-06
929.640	600.000	297.771	290.054	3.67827	6.75857	-.106998E-01	0.200677E-03	0.782351E-06
929.107	605.000	297.784	289.971	3.65024	6.75593	-.108958E-01	0.193940E-03	0.748375E-06
928.574	610.000	297.796	289.888	3.62129	6.75247	-.111060E-01	0.184514E-03	0.703422E-06
928.042	615.000	297.807	289.806	3.59162	6.74831	-.113292E-01	0.173355E-03	0.651605E-06
927.510	620.000	297.818	289.725	3.56130	6.74350	-.115660E-01	0.161139E-03	0.595929E-06
926.978	625.000	297.828	289.644	3.53029	6.73795	-.118195E-01	0.148374E-03	0.538778E-06
926.446	630.000	297.836	289.565	3.49845	6.73146	-.120955E-01	0.135475E-03	0.482297E-06
925.915	635.000	297.843	289.487	3.46549	6.72368	-.124032E-01	0.122840E-03	0.428739E-06
925.384	640.000	297.846	289.412	3.43097	6.71404	-.127571E-01	0.110906E-03	0.380829E-06
924.854	645.000	297.845	289.341	3.39416	6.70169	-.131790E-01	0.100225E-03	0.342202E-06
924.323	650.000	297.839	289.274	3.35440	6.68584	-.136893E-01	0.912908E-04	0.316135E-06
923.793	655.000	297.827	289.210	3.31235	6.66724	-.142686E-01	0.837502E-04	0.299907E-06
923.264	660.000	297.813	289.150	3.26876	6.64681	-.148945E-01	0.771769E-04	0.290252E-06
922.734	665.000	297.797	289.090	3.22414	6.62515	-.155517E-01	0.713003E-04	0.284962E-06
922.205	670.000	297.780	289.032	3.17885	6.60266	-.162302E-01	0.659621E-04	0.282537E-06
921.676	675.000	297.762	288.975	3.13311	6.57963	-.169236E-01	0.610909E-04	0.281935E-06
921.148	680.000	297.743	288.918	3.08709	6.55624	-.176275E-01	0.566904E-04	0.282410E-06
920.619	685.000	297.723	288.862	3.04092	6.53261	-.183396E-01	0.528405E-04	0.283391E-06
920.091	690.000	297.703	288.806	2.99468	6.50885	-.190586E-01	0.497097E-04	0.284386E-06
919.563	695.000	297.682	288.750	2.94846	6.48500	-.197844E-01	0.475827E-04	0.284906E-06
919.036	700.000	297.661	288.695	2.90234	6.46114	-.205182E-01	0.469059E-04	0.284386E-06
918.509	705.000	297.639	288.640	2.85644	6.43731	-.212622E-01	0.483597E-04	0.282094E-06
917.982	710.000	297.616	288.586	2.81089	6.41357	-.220205E-01	0.529681E-04	0.277010E-06
917.455	715.000	297.591	288.532	2.76588	6.39000	-.227993E-01	0.622639E-04	0.267666E-06
916.929	720.000	297.563	288.480	2.72170	6.36668	-.236081E-01	0.785361E-04	0.251905E-06
916.402	725.000	297.532	288.429	2.67876	6.34377	-.244615E-01	0.105191E-03	0.226544E-06
915.876	730.000	297.496	288.380	2.63732	6.32135	-.253682E-01	0.144376E-03	0.189667E-06
915.351	735.000	297.456	288.333	2.59698	6.29929	-.263140E-01	0.192929E-03	0.144546E-06
914.825	740.000	297.415	288.287	2.55738	6.27747	-.272861E-01	0.248089E-03	0.941872E-07
914.300	745.000	297.372	288.242	2.51828	6.25583	-.282758E-01	0.308160E-03	0.407526E-07
913.775	750.000	297.328	288.197	2.47954	6.23430	-.292776E-01	0.372240E-03	0.00000
913.250	755.000	297.283	288.153	2.44104	6.21286	-.302875E-01	0.440071E-03	0.00000
912.725	760.000	297.238	288.109	2.40274	6.19150	-.313031E-01	0.512002E-03	0.00000
912.201	765.000	297.193	288.065	2.36460	6.17021	-.323230E-01	0.589042E-03	0.00000
911.677	770.000	297.147	288.021	2.32661	6.14900	-.333461E-01	0.673025E-03	0.00000
911.153	775.000	297.101	287.977	2.28880	6.12790	-.343722E-01	0.766904E-03	0.00000
910.629	780.000	297.055	287.934	2.25123	6.10694	-.354015E-01	0.875230E-03	0.00000
910.105	785.000	297.009	287.891	2.21397	6.08618	-.364345E-01	0.100488E-02	0.00000
909.582	790.000	296.963	287.848	2.17718	6.06573	-.374726E-01	0.116618E-02	0.00000
909.059	795.000	296.916	287.807	2.14106	6.04571	-.385178E-01	0.137454E-02	0.00000
908.536	800.000	296.869	287.766	2.10594	6.02635	-.395734E-01	0.165299E-02	0.00000
908.013	805.000	296.822	287.727	2.07231	6.00798	-.406442E-01	0.203584E-02	0.169156E-06
907.491	810.000	296.773	287.690	2.04089	5.99105	-.417376E-01	0.257426E-02	0.539301E-06
906.969	815.000	296.724	287.656	2.01261	5.97620	-.428632E-01	0.333434E-02	0.111283E-05
906.447	820.000	296.674	287.626	1.98721	5.96324	-.440181E-01	0.429669E-02	0.187199E-05
905.925	825.000	296.623	287.597	1.96375	5.95157	-.451928E-01	0.539560E-02	0.275647E-05
905.403	830.000	296.572	287.570	1.94159	5.94075	-.463808E-01	0.658600E-02	0.372498E-05
904.882	835.000	296.521	287.544	1.92032	5.93052	-.475778E-01	0.783761E-02	0.474976E-05
904.361	840.000	296.469	287.518	1.89964	5.92067	-.487809E-01	0.913000E-02	0.581212E-05
903.840	845.000	296.417	287.493	1.87937	5.91110	-.499881E-01	0.104493E-01	0.689946E-05
903.319	850.000	296.365	287.468	1.85938	5.90172	-.511981E-01	0.117861E-01	0.800318E-05
902.799	855.000	296.313	287.443	1.83960	5.89247	-.524101E-01	0.131336E-01	0.911732E-05
902.278	860.000	296.261	287.419	1.81999	5.88334	-.536238E-01	0.144869E-01	0.102376E-04
901.758	865.000	296.209	287.394	1.80053	5.87431	-.548387E-01	0.158421E-01	0.113609E-04
901.238	870.000	296.157	287.370	1.78124	5.86539	-.560550E-01	0.171952E-01	0.124842E-04
900.719	875.000	296.105	287.346	1.76213	5.85660	-.572728E-01	0.185424E-01	0.136048E-04
900.199	880.000	296.053	287.322	1.74329	5.84800	-.584925E-01	0.198786E-01	0.147195E-04
899.680	885.000	296.000	287.299	1.72482	5.83966	-.597150E-01	0.211971E-01	0.158241E-04
899.161	890.000	295.948	287.276	1.70689	5.83169	-.609414E-01	0.224881E-01	0.169128E-04
898.642	895.000	295.896	287.254	1.68976	5.82428	-.621736E-01	0.237377E-01	0.179772E-04
898.123	900.000	295.843	287.234	1.67380	5.81770	-.634142E-01	0.249250E-01	0.190050E-04
897.605	905.000	295.790	287.215	1.65960	5.81234	-.646675E-01	0.260194E-01	0.199782E-04
897.086	910.000	295.737	287.199	1.64799	5.80879	-.659395E-01	0.269761E-01	0.208702E-04
896.568	915.000	295.683	287.185	1.63918	5.80721	-.672317E-01	0.277834E-01	0.216742E-04
896.051	920.000	295.629	287.174	1.63233	5.80700	-.685381E-01	0.284862E-01	0.224166E-04
895.533	925.000	295.575	287.165	1.62681	5.80772	-.698540E-01	0.291189E-01	0.231175E-04
895.016	930.000	295.521	287.156	1.62216	5.80905	-.711762E-01	0.297042E-01	0.237905E-04
894.498	935.000	295.467	287.148	1.61811	5.81080	-.725028E-01	0.302577E-01	0.244445E-04
893.981	940.000	295.412	287.140	1.61446	5.81283	-.738322E-01	0.307894E-01	0.250855E-04
893.464	945.000	295.358	287.133	1.61108	5.81505	-.751637E-01	0.313061E-01	0.257171E-04
892.948	950.000	295.303	287.125	1.60789	5.81740	-.764964E-01	0.318119E-01	0.263418E-04
892.431	955.000	295.249	287.118	1.60482	5.81985	-.778302E-01	0.323095E-01	0.269607E-04
891.915	960.000	295.195	287.111	1.60185	5.82237	-.791647E-01	0.327999E-01	0.275741E-04
891.399	965.000	295.140	287.104	1.59895	5.82494	-.804999E-01	0.332833E-01	0.281813E-04

890.883	970.000	295.086	287.098	1.59611	5.82757	-.818357E-01	0.337584E-01	0.287806E-04
890.368	975.000	295.031	287.091	1.59334	5.83027	-.831722E-01	0.342229E-01	0.293692E-04
889.852	980.000	294.977	287.084	1.59064	5.83304	-.845096E-01	0.346725E-01	0.299424E-04
889.337	985.000	294.922	287.078	1.58805	5.83592	-.858484E-01	0.351006E-01	0.304931E-04
888.822	990.000	294.868	287.072	1.58560	5.83896	-.871890E-01	0.354974E-01	0.310105E-04
888.307	995.000	294.814	287.066	1.58336	5.84222	-.885324E-01	0.358476E-01	0.314785E-04
887.793	1000.00	294.760	287.061	1.58142	5.84583	-.898799E-01	0.361287E-01	0.318730E-04

Figure 1 – Simulated 5-meter vertical resolution DFW virtual soundings of pressure (hPa), height AGL (m), temperature (K), dew point temperature (K), u wind component (m/s), v wind component (m/s), w wind component (m/s), turbulence kinetic energy (m^2/s^2), and eddy dissipation rate (m^2/s^3) valid at 1200 UTC 18 September 1997.

3. Simulation Validation

The validation datasets include DFW synthesized wind soundings, which represented a synthesis of DFW wind profiler, lidar, sodar and anemometer observations, as well as 5 m and 40 m observed eddy dissipation rate estimates prepared by the MIT Lincoln Laboratory (e.g., Dasey et al. 1998). The validation procedure included calculating both absolute errors and root mean square errors at times and levels where direct validation data from MIT where available. This required interpolating MIT Lincoln Laboratory sounding datasets to the same vertical resolution as the TAPPS simulated virtual soundings.

Figures 2-13, below, depict tables of averaged absolute errors (absolute values of errors) of u and v wind component up to 600 m AGL, eddy dissipation rate at 40m AGL and turbulence kinetic energy at 40 m AGL over each group of 4 case studies, i.e., the 1200 UTC and 0000 UTC initialized simulations. Only two time periods of observed data were employed to initialize these simulations, which are validated out through 24 hours. These errors are for a very small sample of case studies and represent a point verification for a group of similar weakly-forced large scale environments. Additionally, the MIT profiles may have systematic biases as they represent a synthesis of numerous sensor-derived observations with their own intrinsic biases and errors. The u and v wind component versus height validation (Figures 2-5) represent direct comparison of averaged observations versus averaged simulated fields over each group of 4 case studies at specific heights for all times. The u and v wind component versus time validation (Figures 6-9) represent averaged observations versus averaged simulated fields over each group of 4 case studies for all heights at specific times. Note that the observed datasets were missing at times specified on each diagram. Only 40 m turbulence kinetic energy and eddy dissipation rate errors could be calculated since the 5 m simulated fields were not available due to their being below the first model level of ~7 m AGL.

Specific findings of these small numbers of case studies can be summarized by the following general conclusions concerning u and v wind component errors versus height and time:

1) The u component errors exhibited little height dependence while the v component errors exhibited significant relative height dependence from both groups.

2) The 1200 UTC initialized u and v component errors were much smaller than the 0000 UTC initialized u and v component errors versus height and time.
3) The u and v component errors are similar in magnitude when initialized at 1200 UTC but the v component is much larger than the u component wind error initialized at 0000 UTC.
4) The maximum error with respect to height for both groups and both components is at ~400 m +- ~100 m AGL.
5) The maximum error with respect to time for both groups is during the midafternoon period.
6) Both the u and v wind components exhibited double temporal error maxima from the 0000 UTC initialized simulations but only a single temporal maxima from the 1200 UTC simulations.
7) The u and v components exhibited a double temporal minima in the 1200 UTC simulations but not in the 0000 UTC simulations where a single temporal minima occurred.

As far as eddy dissipation rate and turbulence kinetic energy errors are concerned (note Figures 10-13):

1) Eddy dissipation rate errors peak ~10^{-2} m^2/s^3 after the first 30 minute period but then drop to ~10^{-3} m^2/s^3 for the remainder of the simulation for both groups.
2) Turbulence kinetic energy errors are consistent with wind component errors in terms of their temporal variation.

The most important general and preliminary findings to be derived from these experiments are the following:

1) 1200 UTC initial data enabled a much more accurate simulation of nocturnally-forced boundary layer jets as well as, possibly, the background synoptic flow regime at DFW. This is likely because the 1200 UTC large scale analyses contained more of a signal of these boundary layer features, in particular, which had not developed at 0000 UTC and where, therefore absent from the larger scale initial datasets at 0000 UTC. May also be, in part, a result of the times of the availability of observations.

2) The v wind component variance is much more pronounced in the lower troposphere for nocturnal boundary layer jets than is the u wind component variance.

3) The simulation of stable boundary layer may lend itself to deterministic simulation better than the convective boundary layer does as errors tended to peak during the period of most significant surface sensible heating and convective overturning within the boundary layer.

4) Eddy dissipation rate simulation is likely very sensitive to the initial data and initial data adjustment processes employed in a deterministic numerical model as these

errors peaked right after model initialization. Overall these errors were very large but are likely highly sensitive to the formulation employed for both the observations and simulations reflecting differences in these formulations.

5) The most frequent level of the nocturnal boundary level jets at DFW is ~400 m AGL.

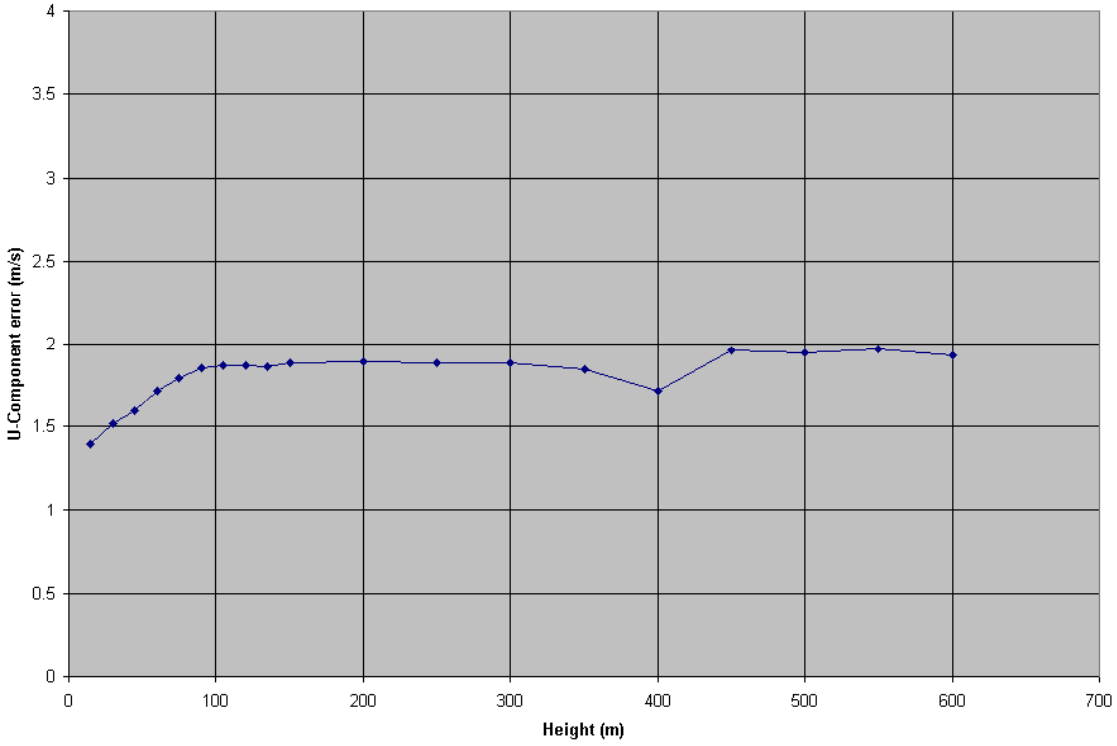

Figure 2 – Simulated averaged u wind component errors (m/s) versus height (m AGL) from the 1200 UTC initial data.

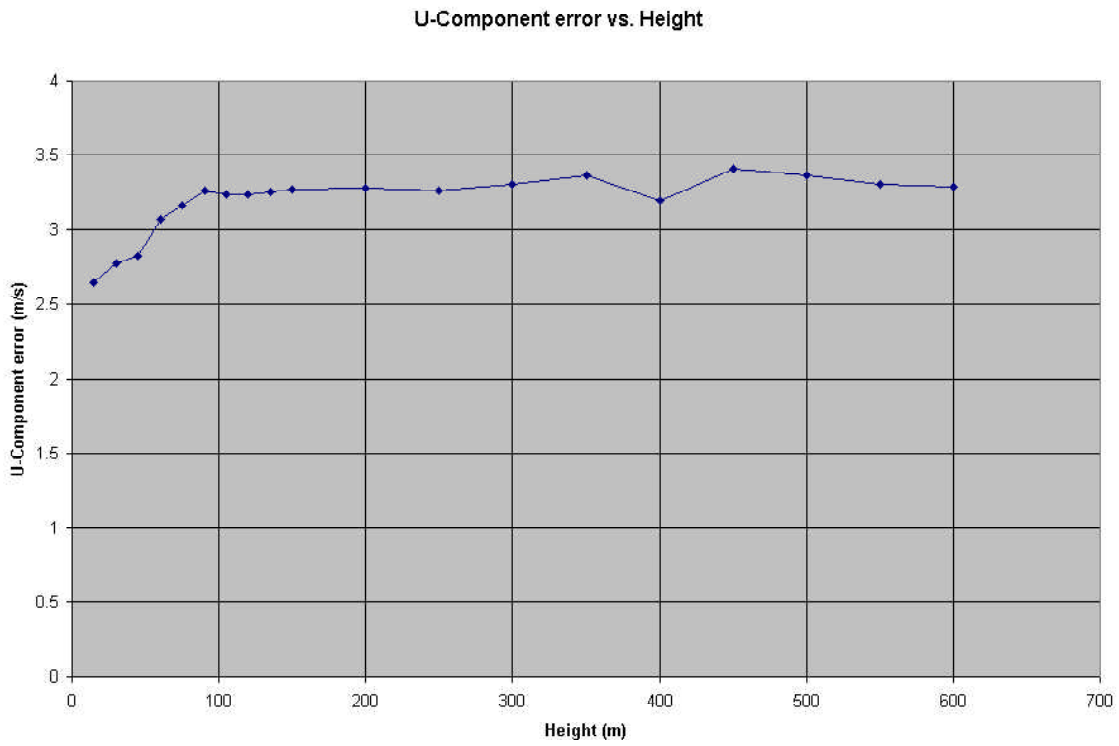

Figure 3 – Simulated averaged u wind component error (m/s) versus height (m AGL) from the 0000 UTC initial data.

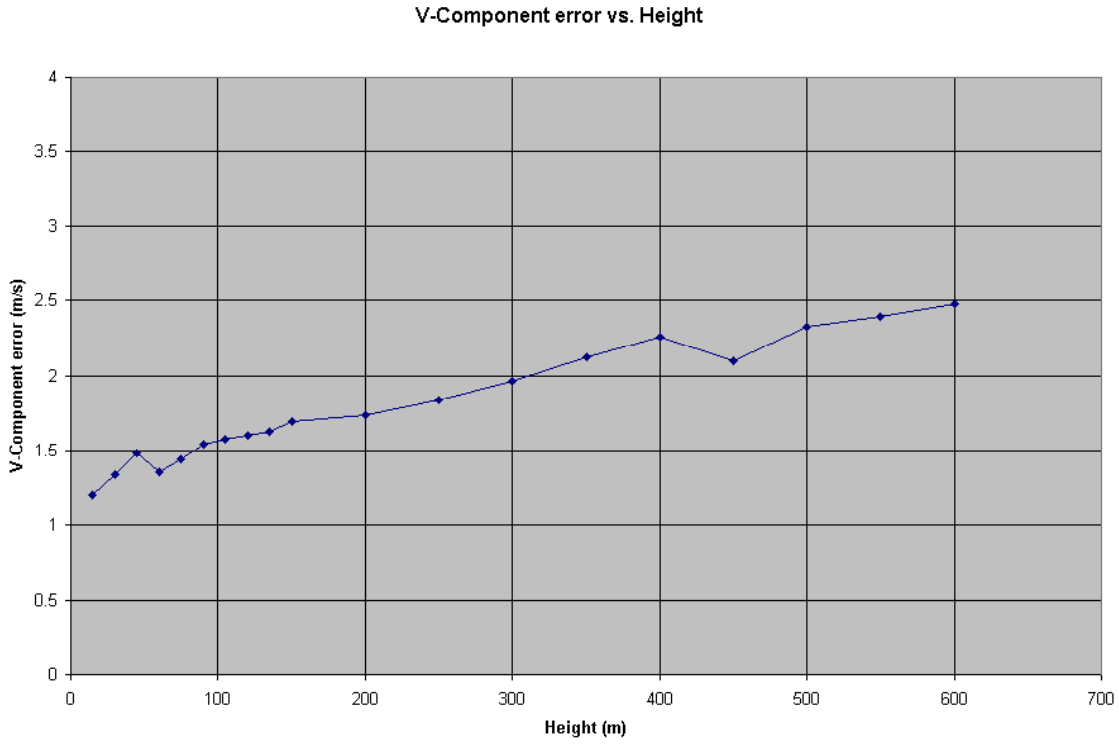

Figure 4 – Simulated averaged v wind component error (m/s) versus height (m AGL) from the 1200 UTC initial data.

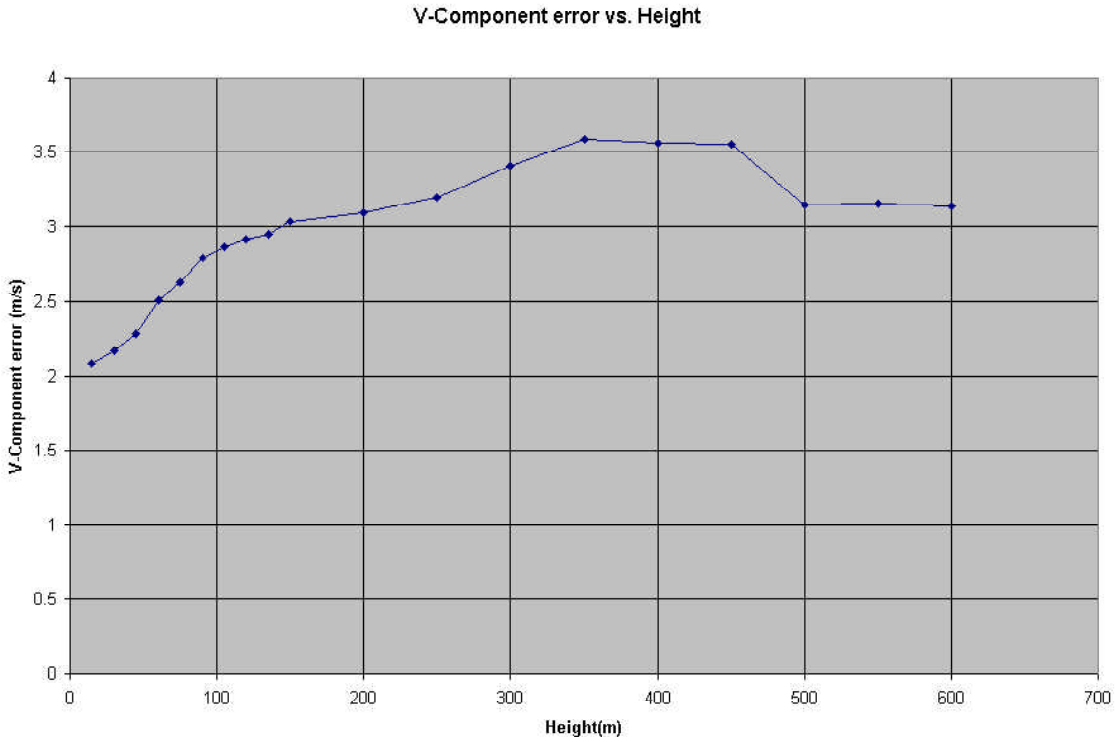

Figure 5 – Simulated averaged v wind component error (m/s) versus height (m AGL) from the 0000 UTC initial data.

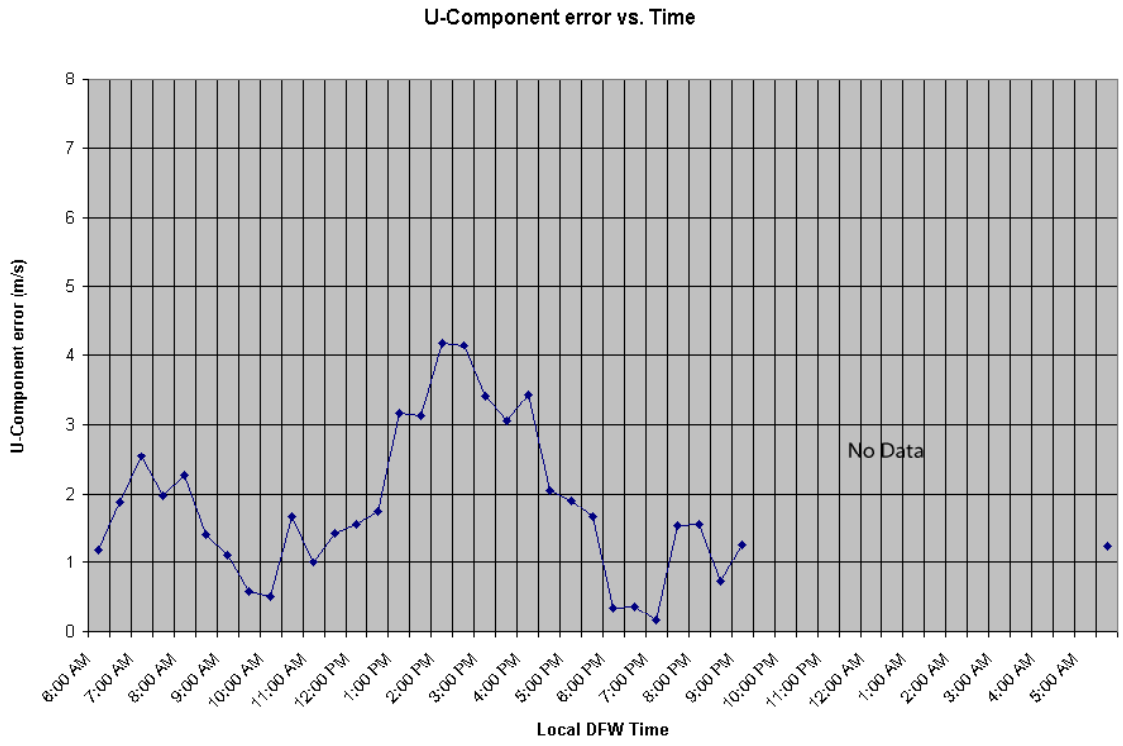

Figure 6 – Simulated averaged u wind component error (m/s) versus time (hr) from the 1200 UTC initial data.

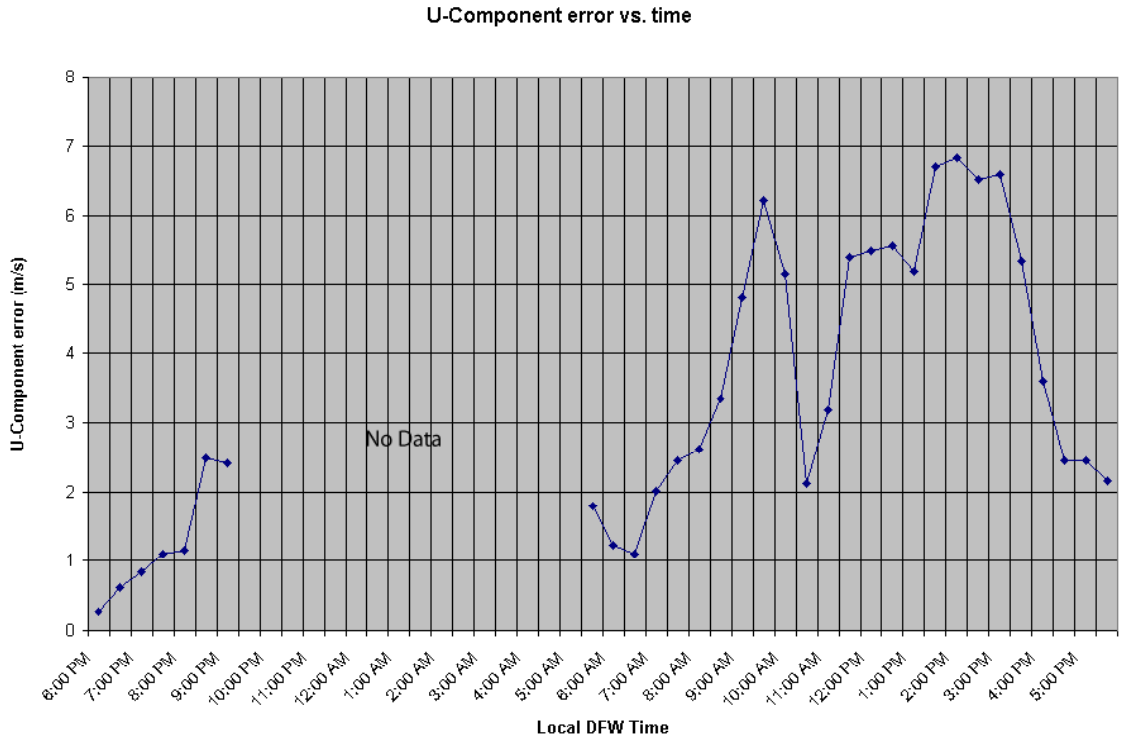

Figure 7 – Simulated averaged u wind component error (m/s) versus time (hr) from the 0000 UTC initial data.

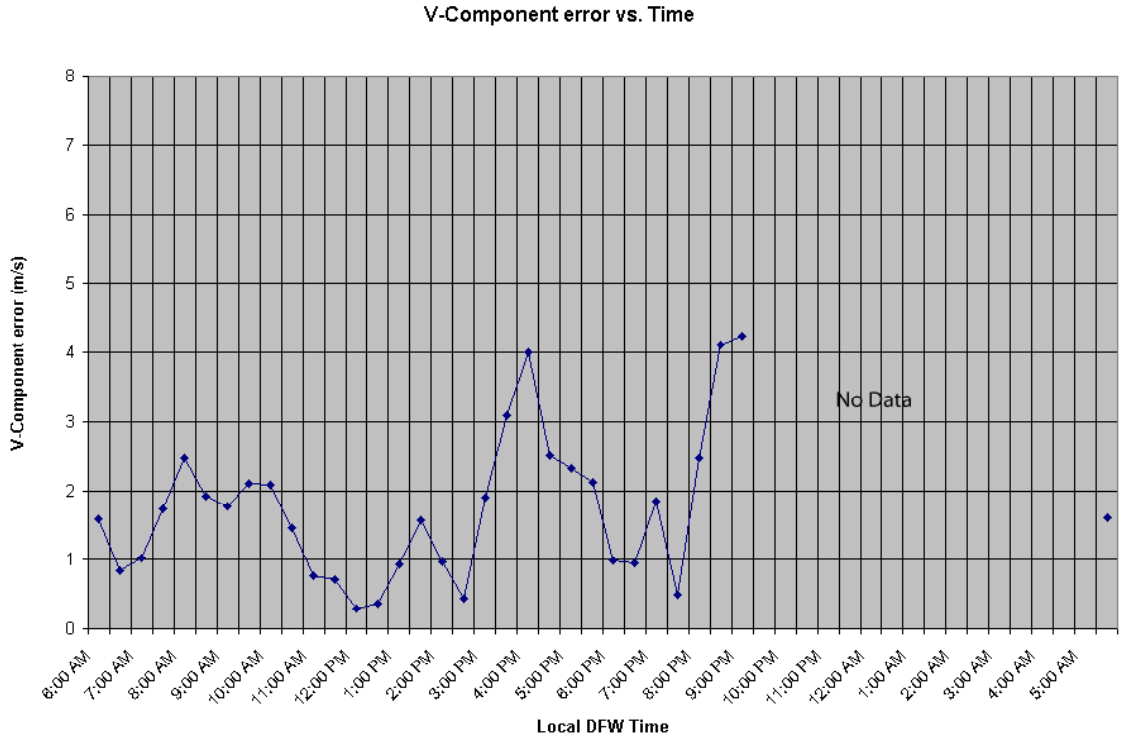

Figure 8 – Simulated averaged v wind component error (m/s) versus time (hr) from the 1200 UTC initial data.

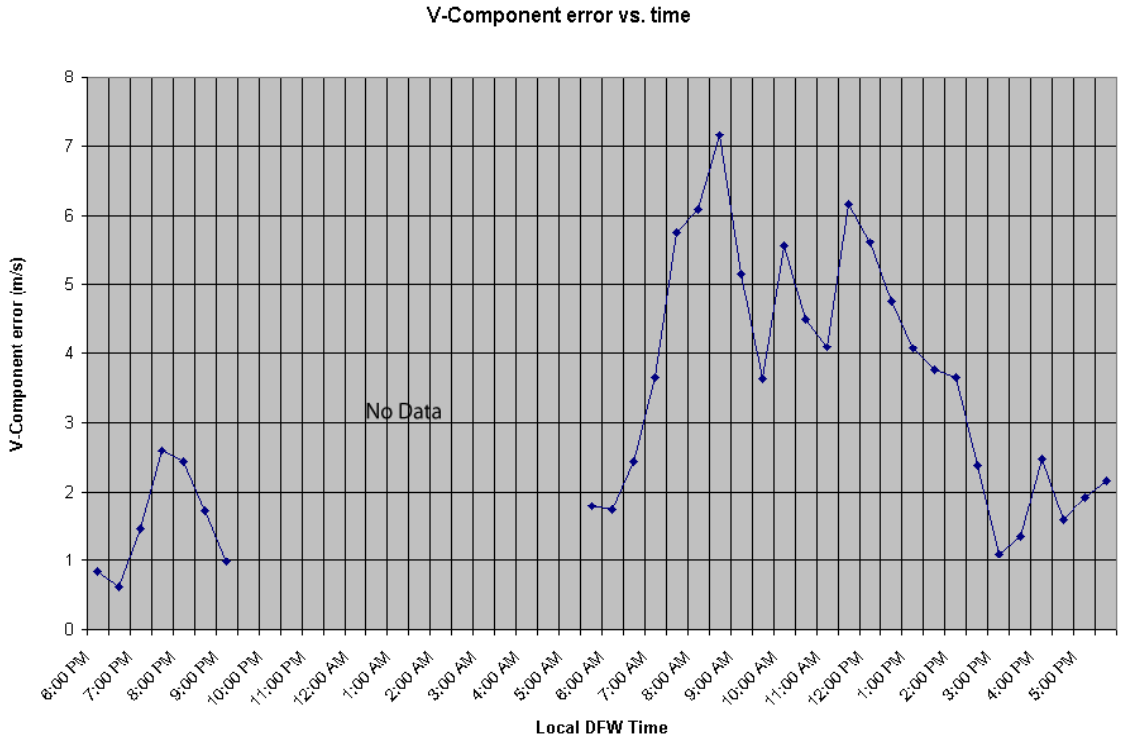

Figure 9 – Simulated averaged v wind component error (m/s) versus time (hr) from the 0000 UTC initial data.

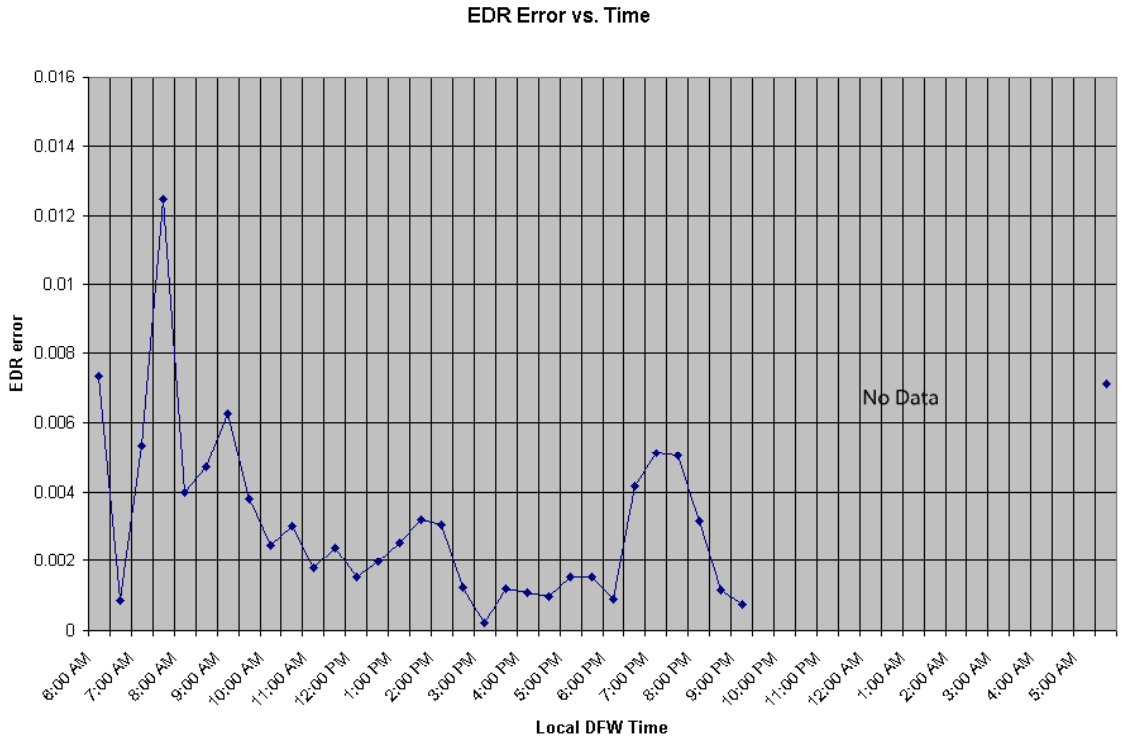

Figure 10 – Simulated averaged eddy dissipation rate error (m^2/s^3) versus time (hr) at 40 m AGL from the 1200 UTC initial data.

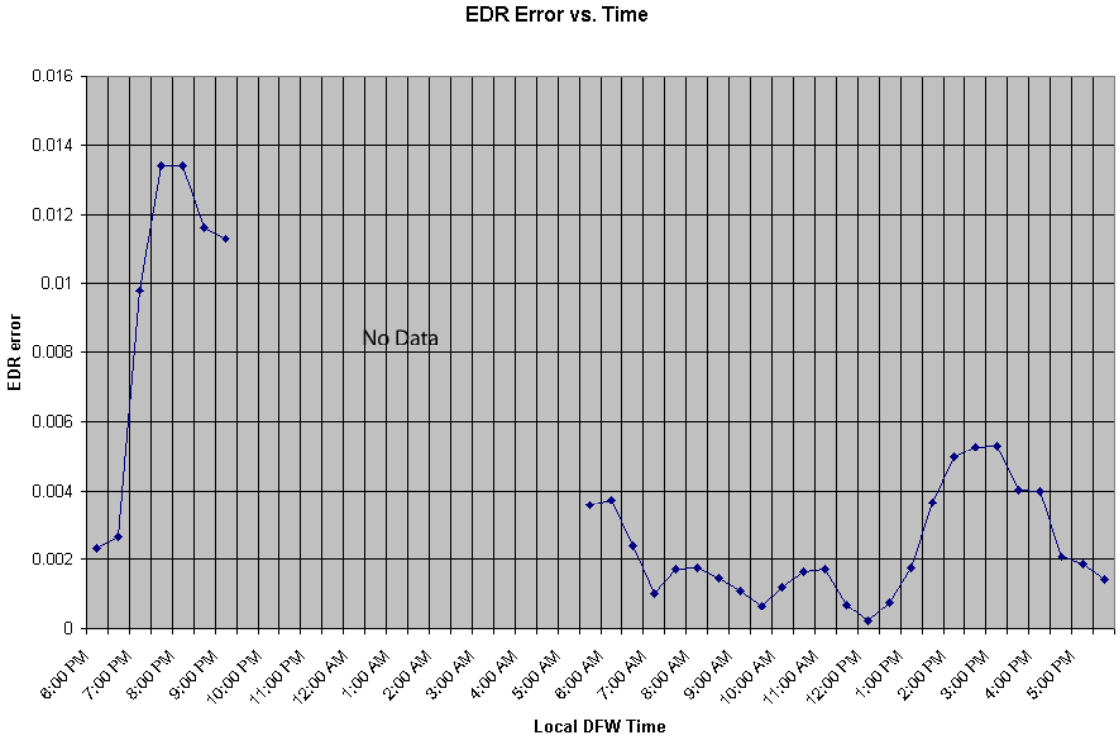

Figure 11 – Simulated averaged eddy dissipation rate error (m^2/s^3) versus time at 40 m AGL from the 0000 UTC initial data.

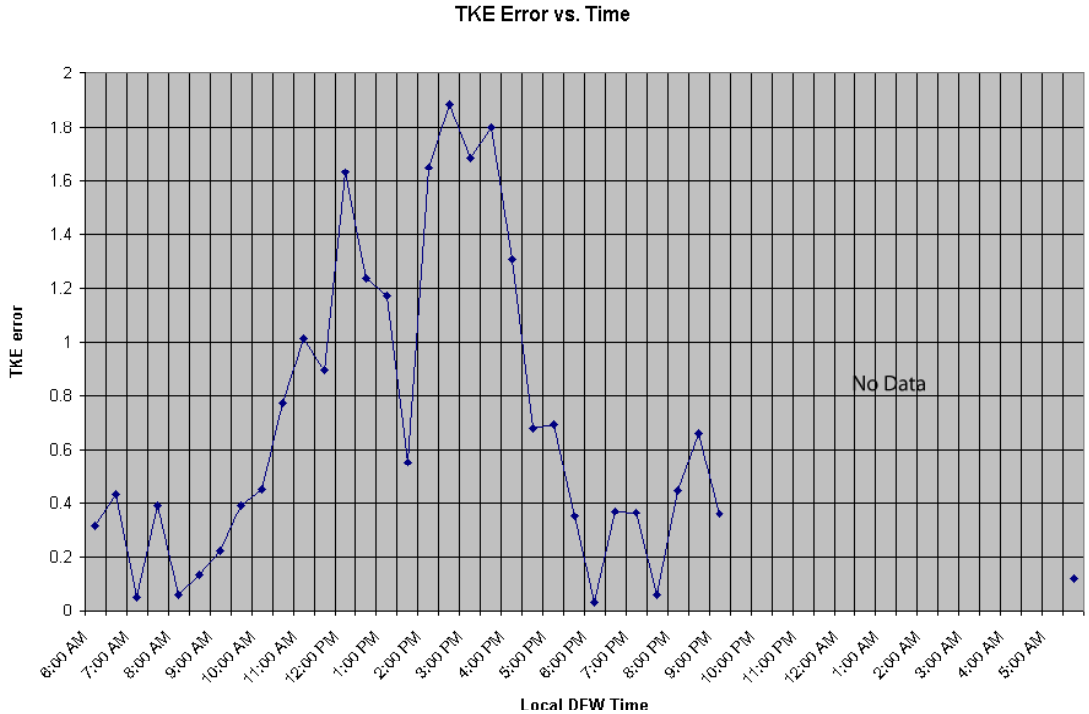

Figure 12 – Simulated averaged turbulence kinetic energy error (m^2/s^2) versus time at 40 m AGL from the 1200 UTC initial data.

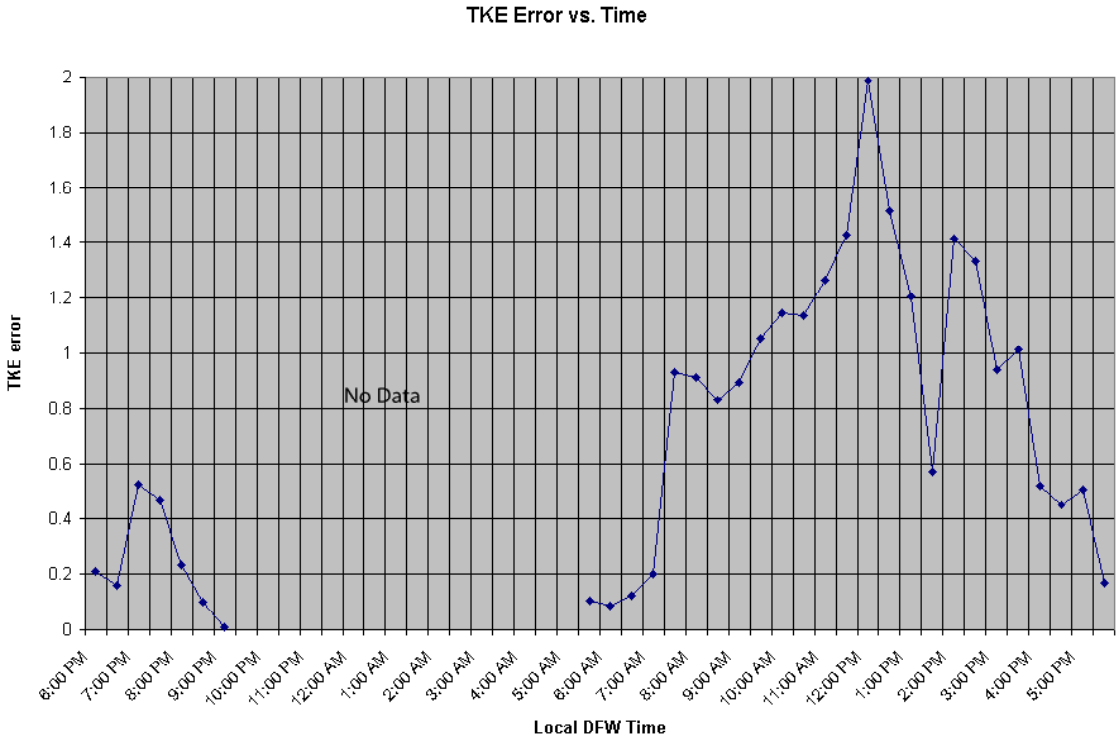

Figure 13 – Simulated averaged turbulence kinetic energy error (m^2/s^2) versus time at 40 m AGL from the 0000 UTC initial data.

4. References

Anderson, J. R., E. E. Hardy, J. T. Roach and R. E. Witmer, 1976: A land use and land cover classification system for use with remote sensor data. U.S. Geological Survey Professional Paper 964, U. S. Government Printing Office, Washington, DC, 28 pp. [Available from U.S. Government Printing Office, Washington, DC 20402].

Bougeault, P., and P. Lacarrere, 1989: Parameterization of orography-induced turbulence in a mesobeta-scale model. Mon. Wea. Rev., 117, 1872-1890.

Dasey, T. J., R. E. Cole, R. M. Heinrichs, M. P. Mathews and G. H. Perras, 1998: Aircraft Vortex Spacing System (AVOSS) initial 1997 system deployment at Dallas-Fort Worth (DFW) airport. Project Rep. NASA/L-3, 68 pp. [Available from MIT Lincoln Laboratory, Lexington, MA 02420].

Kain, J. S., and J. M. Fritsch, 1992: A one-dimensional entraining/detraining plume model. J. Atmos. Sci., 47, 2784-2802.

Kaplan, M. L., Y.-L. Lin, J. J. Charney, K. D. Pfeiffer, D. B. Ensley, D. S. DeCroix and

R. P. Weglarz, 2000: A Terminal Area PBL Prediction System at Dallas-Fort Worth and its application in simulating diurnal PBL jets. Bull. Amer. Meteor. Soc., 81, 2179-2204.

Mahrt, L., and H. Pan, 1984: A two-layer model of soil hydrology. Bound.-Layer Meteor.,29, 1-20.

Noilan. J., and S. Planton, 1989: A simple parameterization of land surface processesfor meteorological models. Mon. Wea. Rev., 117, 536-549.

Therry, G., and P. Lacarrere, 1983: Improving the eddy kinetic energy model for the planetary boundary layer. Bound-Layer Meteor., 25, 63-88.